Nanoscale

Dissipative Self-Assembly of a Proline Catalyst for Temporal Regulation of the Aldol Reaction

Journal:	*Nanoscale*
Manuscript ID	NR-ART-07-2022-003991.R1
Article Type:	Paper
Date Submitted by the Author:	20-Sep-2022
Complete List of Authors:	Reardon, Thomas; The Ohio State University Na, Baichuan; The Ohio State University, Chemistry and Biochemistry Parquette, Jon; The Ohio State University

SCHOLARONE™
Manuscripts

Article

Received 00th January 20xx,
Accepted 00th January 20xx

DOI: 10.1039/x0xx00000x

Dissipative Self-Assembly of a Proline Catalyst for Temporal Regulation of the Aldol Reaction

*Thomas J. Reardon,[a] Baichuan Na[a] and Jon R. Parquette[a]**

The spatiotemporal regulation of chemical reactivity in biological systems permits a network of metabolic reactions to take place within the same cellular environment. The exquisite control of reactivity is often mediated by out-of-equilibrium structures that remain functional only as long as fuel is present to maintain the higher energy, active state. An important goal in supramolecular chemistry aims to develop functional, energy dissipating systems that approach the sophistication of biological machinery. The challenge is to create strategies that couple the energy consumption needed to promote a molecule to a higher energy, assembled state to a functional property such as catalytic activity. In this work, we demonstrated that the assembly of a spiropyran (SP) dipeptide (**1**) transiently promoted the proline-catalyzed aldol reaction in water when visible light was present as fuel. The transient catalytic activity emerged from **1** under light illumination due to the photoisomerization of the monomeric, *O*-protonated (**1**-MCH$^+$) merocyanine form to the spiropyran (**1**-SP) state, which rapidly assembled into nanosheets capable of catalyzing the aldol reaction in water. When the light source was removed, thermal isomerization to the more stable MCH$^+$ form caused the nanosheets to dissociate into a catalytically inactive, monomeric state. Under these conditions, the aldol reaction could be repeatedly activated and deactivated by switching the light source on and off.

Introduction.

Biological systems regulate complex networks of chemical reactions associated with cellular metabolism via the local activation and spatial confinement of proteins in the cell.[1,2] The spatial and temporal regulation of protein function is critical to separate incompatible chemical reactions within the highly interconnected network of metabolic processes that must take place in the same environment. This control over chemical reactivity emerges from out-of-equilibrium structures that persist only as long as energy is continuously dissipated.[3] The energy that flows through these structures often induces the components to self-organize into a dynamically interacting system that acquires emergent properties or functions.[4] These processes produce the concentration gradients and feedback loops in cells that allow for work to be accomplished and biological functions to be efficiently regulated. Although many strategies have been developed to couple energy consumption to the assembly of ordered, non-equilibrium structures, few of these systems exhibit controllable functions, which have potential to integrate with a larger, networked system.[5-16] Recently, a transient microgel that autonomously regulated its lifetime using chemical feedback coupled to the self-assembly process has been reported.[17] An important step to advance the field toward chemical systems that replicate biological networks will be to develop strategies to utilize fuel-driven assembly to regulate chemical reactivity.

The challenge lies in coupling the energy consumption used to promote a component into a higher energy, nonequilibrium steady state with a transient functional property, such as catalysis.[18] Amphiphilic materials, such as micelles, provide nonpolar regions that accelerate the reaction of water-insoluble reactants via the hydrophobic effect in water.[19] Consequently, recent examples have exploited the fuel-driven, self-assembly of amphiphilic assemblies to accelerate bimolecular processes, such displacement or cycloaddition reactions, by transient confinement of the reactants.[20-24] Dissipative systems that couple light-driven modulation of nanoparticle surface composition to transient changes in catalytic activity have also been reported.[25-27] In this work, we demonstrate that the assembly of a spiropyran (SP) dipeptide **1** (Pro-Lys (SP)) transiently promotes the proline-catalyzed aldol reaction in water by sequestering the catalytic site within a hydrophobic microenvironment when light is present as fuel.

We have previously shown that nanotubes formed by the self-assembly of a Pro-Lys dipeptide catalyzed the aldol condensation in water, but that activity terminated upon dissociation of the nanotube.[28] L-Proline catalyzes the direct aldol reaction between ketones and aldehydes in organic solvents, but proceeds poorly in water.[29] The amphiphilic nanotube structure served to sequester the organocatalytic site from the aqueous phase, which accelerated the proline-catalyzed aldol reaction in water.[30-33] Based on that precedent, we hypothesized that the aldol reaction could be transiently catalyzed using an analogous proline-containing peptide capable of undergoing dissipative self-assembly into a nanostructure that sequestered the active site in aqueous media. Recently, we demonstrated that a spiropyran chromophore could function as a

[a] *Department of Chemistry and Biochemistry*
The Ohio State University
100 W. 18th Ave. Columbus, Ohio 43210
E-mail: parquette.1@osu.edu
Electronic Supplementary Information (ESI) available

Article

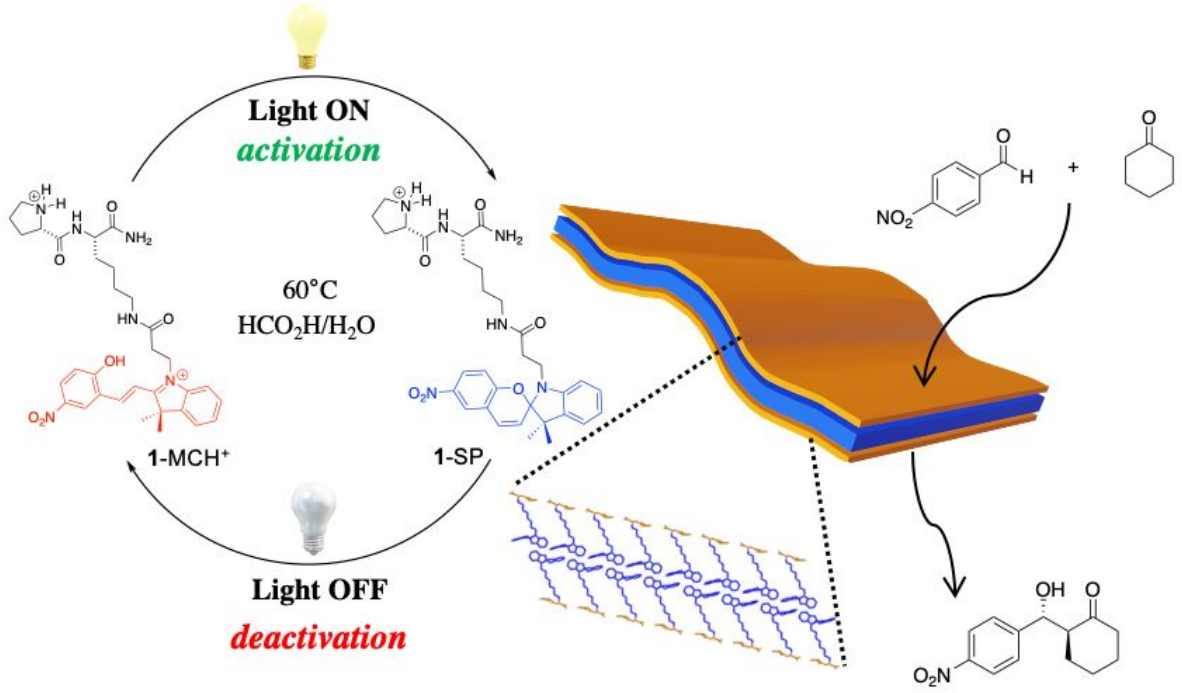

Figure 1. Transient self-assembly of catalytic nanosheets of Pro-Lys (SP) **1** driven by visible light as fuel. Scheme showing the aldol reaction of 4-nitrobenzaldehyde and cyclohexane, catalyzed by nanosheets of Pro-Lys(SP) **1,** which assembled in the presence of visible light.

switch to modulate the overall amphiphilicity and self-assembly of a peptide.[34] This peptide assembled into a transient nanofiber hydrogel in the presence of visible light and dissociated when the light source was removed. Accordingly, Pro-Lys dipeptide **1**, was designed with a catalytic proline residue along with a spiropyran chromophore appended to the lysine residue at the ε-amino position (Fig. 1). The juxtaposition of the nonpolar spiropyran chromophore with the positively charged peptide sequence induced the amphiphilicity required to drive peptide self-assembly in water. Spiropyrans reversibly interconvert between a nonpolar spiropyran (SP) form and a zwitterionic, merocyanine (MC) form, which displays a comparatively large electric dipole moment that would decrease the amphiphilicity of the monomer and dissociate the assembly.[35] In water at low pH values, the zwitterionic (MC) or *O*-protonated (MCH^+) form is thermodynamically most stable and thermal isomerization often occurs spontaneously.[36] Therefore, the SP→MCH^+ interconversion was envisioned as mechanism to modulate the assembly state and catalytic activity of peptide **1** using light as fuel.

Results and Discussion

The dipeptide (Pro-Lys (SP), **1**) was prepared using Fmoc solid-phase chemistry on Rink amide resin, whereby the spiropyran chromophore was installed by on-bead amidation of the ε-amino lysine sidechain after deprotection of the MTT group of the resin-bound (Fmoc)Pro-Lys(MTT) dipeptide (Scheme S1). The photoresponsive behavior of **1** was initially investigated by UV-Vis spectroscopy in water with added trifluoroacetic acid (TFA) (Fig. 2). In aqueous TFA (10 mM), the spiropyran (**1**-SP) and *O*-protonated merocyanine (**1**-MCH^+) forms exhibited characteristic UV absorptions at 351 and 410 nm, respectively (Fig. 2a). Irradiation of an aqueous solution of **1** (0.5 mM, 10 mM TFA) with broad-spectrum visible light (72 W, 3600 lumens) converted the **1**-MCH^+/SP mixture to the SP isomer, extinguishing the broad absorption at 410 nm within 5 min. Thermal isomerization of **1**-SP to **1**-MCH^+ in water (10 mM TFA) proceeded to completion in 10-15 min at 60°C, 35-40 min at 50°C and ~2 h at 40°C (Fig. 2b). It is noteworthy that irradiation with visible light efficiently isomerized **1**-MCH^+ (0.5 mM, 10 mM TFA) to >99% **1**-SP within 5 min., even at 60°C, indicating that photochemical ring-closure could overwhelm the competing thermal ring-opening process. The ability of **1**-SP and **1**-MCH^+ to undergo self-assembly under static conditions in water was then explored by transmission electron microscopy (TEM). Thus, an aqueous solution (1 mM, 10 mM TFA) of **1** was isomerized to **1**-MCH^+ by heating to 60°C in the dark for 30 min, then incubated for 24 h at 22°C. TEM imaging of the sample confirmed that no discernible structures were produced by **1**-MCH^+ under these conditions (Fig. 2d). In contrast, a solution of **1**-MCH^+ in water (1 mM, 10 mM TFA), under continuous visible light irradiation at 22°C for 24 h produced 2-D, sheet-like assemblies, as observed by TEM imaging (Fig. 2c).

The open and closed states of **1** (**1**-SP and **1**-MCH^+) were independently evaluated as catalysts for the aldol reaction of *p*-

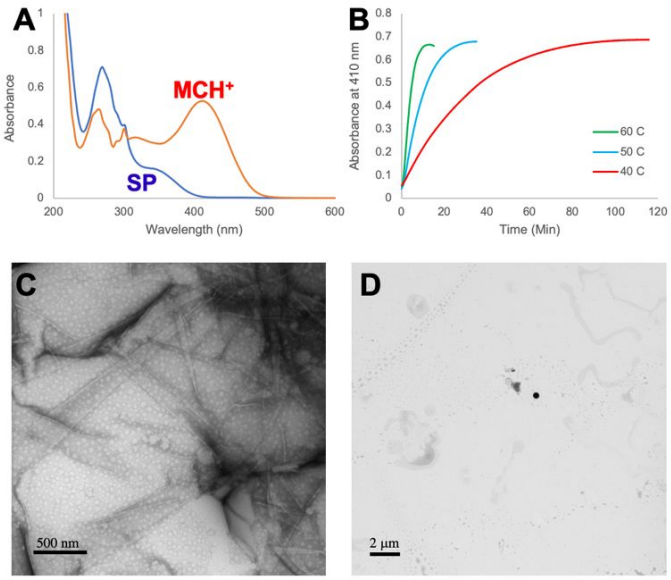

Figure 2. Interconversion of merocyanine and spiropyran forms of **1** in water (0.5 mM, 10 mM TFA), as monitored by the increase/decrease of the MCH$^+$ absorption at 410 nm. (A) UV-Vis spectra of **1** after heating at 60°C in the dark for 45 min, producing absorption at 410 nm, characteristic of **1**-MCH$^+$, and after exposure to visible light at 60°C for 5 min., which extinguished the 410 nm absorption. (B) Time-dependent absorption at 410 nm as a function of temperature, reflecting the thermal isomerization of **1**-SP to **1**-MCH$^+$. TEM images of **1** in water (1 mM, 10 mM TFA) (C) after irradiation with visible light for 24 h in water; and (D) after heating to 60°C for 30 min in the dark.

Table 1. Initial optimization of the on/off conversion ratio of the aldol reaction of 4-nitrobenzaldehyde and cyclohexanone under static conditions.[a]

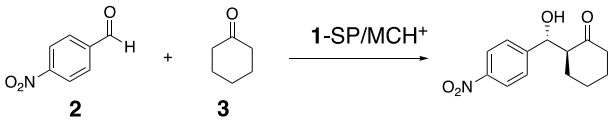

	Light	Load (mol %)	Acid (10 mM)	Time (h)	Temp (°C)	Ratio (**3**/**2**)	Conv.[b] (%)	dr[c] (*Syn*:*Anti*)
1	**ON**	10	TFA	16	40	10:1	71	1:3.5
2	OFF	10	TFA	16	40	10:1	20	1:4.0
3	**ON**	10	TFA	72	40	10:1	82	1:1.7
4	OFF	10	TFA	72	40	10:1	70	1:5.4
5	**ON**	5	TFA	16	40	10:1	40	1:10
6	OFF	5	TFA	16	40	10:1	9	1:2.0
7	**ON**	15	TFA	16	40	10:1	75	1:4.9
8	OFF	15	TFA	16	40	10:1	42	1.5.4
9	**ON**	10	AcOH	16	22	10:1	79	1:17
10	OFF	10	AcOH	16	22	10:1	3	--
11	**ON**	10	AcOH	16	40	10:1	91	1:10
12	OFF	10	AcOH	16	40	10:1	97	1:8.0
13	**ON**	10	AcOH	16	40	5:1	92	1:8.3
14	OFF	10	AcOH	16	40	5:1	94	1:8.3
15	**ON**	5	AcOH	16	40	5:1	92	1:8.2
16	OFF	5	AcOH	16	40	5:1	18	1:7.5
17	**ON**	5	AcOH	16	60	5:1	99	1:3.6
18	OFF	5	AcOH	16	60	5:1	79	1:3.4

(a) Reactions were performed using *p*-nitrobenzaldehyde (1 equiv.), cyclohexanone (5-10 equiv.), dipeptide **1** (5-15 mol%) and acid additive in water (10 mM). (b) Conversion of aldehyde into aldol product, determined by ^{1}H NMR spectroscopy. (c) Determined by ^{1}H NMR spectroscopy.

nitrobenzaldehyde with cyclohexanone in acidic water (10 mM TFA) at 40°C, using a 10-fold excess of cyclohexanone (Table 1, entries 1-8). Accordingly, using 10 mol% **1**-SP under continuous irradiation with broad spectrum light at 40°C to maintain the closed spiropyran state, 71% conversion to aldol product was achieved after 16 h. In contrast, employing 10 mol% **1**-MCH$^+$ as catalyst at 40°C in the absence of light produced only 20 % conversion after the same amount of time. Although the moderate difference in conversion mediated by **1**-SP and **1**-MCH$^+$ supported the role of self-assembly in determining catalytic activity, after 72 h, this difference eroded, affording 82 and 70% conversions for **1**-SP and **1**-MCH$^+$, respectively (entries 1-4). After evaluating a wide range of conditions, several parameters of the reaction were found to have a significant impact on the relative activity of the two forms of **1**. (1) Lowering the catalyst loading level caused an increase in activity of **1**-SP over **1**-MCH$^+$, consistent with reduced aggregation of **1**-MCH$^+$ at the lower catalyst concentration (entries 5-8, 13-16). (2) Replacing TFA with acetic acid enhanced catalyst activity at lower temperature, which might be attributed to the lower comparative acidity of acetic acid.[37] Thus, at 22°C, **1**-SP and **1**-MCH$^+$ produced 70 and 3% yields of aldol products, respectively; however, the reactivity difference significantly diminished at 40°C (entries 9-12). (3) Performing the reaction at elevated temperatures increased the activity of **1**-MCH$^+$ (entries 9-12; 15-18). (4) Increasing the acetic acid concentration from 10 to 50 mM, increased the reactivity difference. (Table 2, entries 3-4).

Based on these observations, the optimal conditions to enhance the differential activity **1**-SP and **1**-MCH$^+$ would employ 5 mol% catalyst and 50 mM acetic acid, using a 5-fold excess of cyclohexanone at lower temperatures. However, the ability to transiently activate the catalyst with light irradiation requires the reversible assembly of **1**-SP into an active form that rapidly dissociates when the light is turned off. Thus, the reaction must be conducted at elevated temperatures to ensure the rapid conversion of **1**-SP to **1**-MCH$^+$ when the light source was removed. However, as noted in Table 1, performing the reaction at elevated temperatures increased the activity of **1**-MCH$^+$ (entries 9-12; 15-18), which reduced the k_{on}/k_{off} rate ratio. We reasoned that the difference in assembly properties of the two states of **1**, and the corresponding k_{on}/k_{off} ratio, could be optimized by varying the carboxylate counterion formed by protonation of the proline residue in **1** by the added acid. This supposition was suggested by prior work showing that the carboxylate counterions ion-paired to the lysine residue of a related spiropyran peptide critically impacted hydrogel assembly [34] In particular, trifluoroacetate counterions greatly enhanced self-assembly, compared with other less lipophilic carboxylates, due to the capability of trifluoroacetates to increase the overall hydrophobicity of peptides in water.[38,39]

Table 2. Effect of acid additive on aldol reaction of **2** and **3** at 60°C.

	Light Cond.[a] (ON/OFF)	Acid (mM)	Conv.[b] (%)	*dr*[c] (Syn:Anti)	ee^{d}_{anti} (%)
1	**ON**	HCO_2H	89	1:2.7	73
2	OFF	HCO_2H	9	1:3.0	68
3	**ON**	CH_3CO_2H	94	1:2.3	54
4	OFF	CH_3CO_2H	27	1:2.8	78
5	**ON**	$C_2H_5CO_2H$	97	1:2.3	60
6	OFF	$C_2H_5CO_2H$	90	1:2.8	84
7	**ON**	$C_3H_7CO_2H$	99	1:1.8	48
8	OFF	$C_3H_7CO_2H$	99	1:2.1	78

(a) Reactions were performed using *p*-nitrobenzaldehyde (**2**) (1 equiv.), cyclohexanone (**3**) (5 equiv.), dipeptide **1** (5 mol%) and acid additive (50 mM) in water at 60°C. (b) Conversion of aldehyde into aldol product, determined by ^{1}H NMR spectroscopy. (c) Determined by ^{1}H NMR spectroscopy. (d) Measured by HPLC on a chiral stationary phase (AD-RH Diacel Chiralpak, 20% *i*-PrOH/hexane, UV 254 nm, Flow rate 1.0 mL/min).

Accordingly, we surveyed reaction conditions at 60°C that varied the acid additives (50 mM) under the optimal conditions (Table 2). These studies revealed that formic acid produced the largest difference in conversion between **1**-SP and **1**-MCH$^+$, which progressively decreased going from formic acid to butyric acid. The reaction rates and selectivities under light-on conditions were comparable to those of previously reported hydrophobically modified, proline catalysts.[40] The self-assembly of **1**-SP produced nanosheets and the thermal isomerization process occurred efficiently for all the acids in Table 2, similar to conditions using TFA as additive (Figs. S4-7). Dynamic light scattering in water (0.5 mM) showed significantly higher molar scattering intensities for **1** under light irradiation at 60°C, compared with the intensities measured in the dark (Table S1). However, under dark conditions, the low scattering intensities, and the degree of aggregation observable by TEM imaging, did not increase with acid lipophilicity, as would be expected for increased aggregation of **1**-MCH$^+$ (Figs. S6-7). The lower k_{on}/k_{off} ratios measured for more lipophilic acids may have emerged from the ability of the additive to provide a separate hydrophobic environment for the reaction, which would be minimal for formic acid.

The self-assembly characteristics of the catalyst were further evaluated in water (5 mol%, 5 mM) in the presence of 50 mM formic acid at 60°C under intermittent light-on and light-off conditions (Fig. 3a-d). After 2 h at 60°C under continuous irradiation with visible light, TEM imaging showed the formation of nanosheets. In contrast, removing the light source at 60°C caused the nanosheets to dissociate, as evidenced by the lack of any observable structures by TEM. Monitoring two cycles of nanosheet assembly and disassembly induced at 60°C by turning the light source on and off in 2 h intervals confirmed that the process was dynamic and durable under the reaction conditions. After six light-on (5 min) /off (40 min) cycles at 60°C, a ~17% decrease in the amplitude of the **1**-MCH$^+$ absorption was observed at 405 nm (Fig. S8), likely due to photobleaching of the SP/MCH$^+$ chromophore. The state of **1** at 60°C was also evaluated by dynamic light scattering under light-on and light-off conditions, which exhibited molar scattering

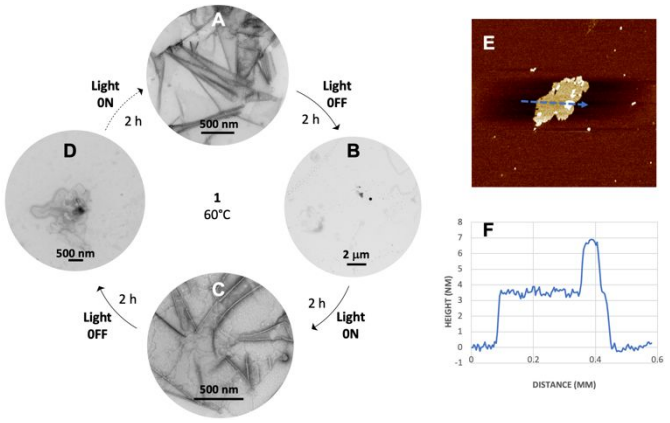

Figure 3. Interconversion of **1**-SP and **1**-MCH$^+$ under dynamic conditions (water, 60°C, HCO_2H (50 mM), **1** (5 mol%, 5 mM)). (A-D) TEM images of **1** (5 mM) in water (50 mM HCO_2H) at 60°C after two light ON-OFF cycles, performed at 2 h intervals. (E) AFM image of **1** (5 mM) in water (50 mM HCO_2H) at 60 °C after 2 h of visible light irradiation. (F) Cross-sectional height profile measured from the image along the dotted blue arrow. AFM image of **1**-SP was recorded at ambient temperature in tapping mode on freshly cleaved mica. Sample was prepared by diluting a 5 mM sample to 0.5 mM and cooling to ambient temperature for analysis.

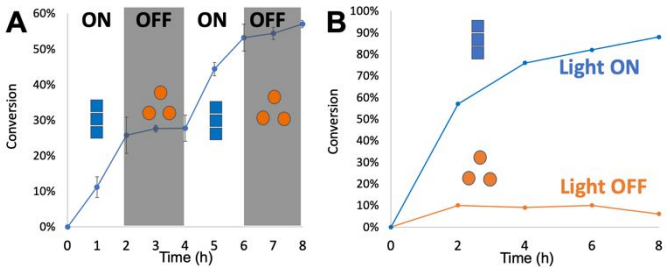

Figure 4. Demonstration of transient catalytic activity of **1** under dynamic conditions (60°C, water (50 mm HCO_2H, **1** (5 mol%, 5 mM)) with the (A) light switched on and off in 2 h intervals and under (B) static conditions. All data points were taken from separate reactions run in parallel due to the inhomogeneous nature of the reaction mixture, which precluded obtaining reproducible aliquots for analysis. Conversions measured by using diagnostic peaks by ^{1}H NMR.

intensities with derived count rates of 451 ± 8 and 85 ± 26 10^4 counts s^{-1} M^{-1}, respectively. Cross-sectional height analysis of the nanosheets formed under these conditions by atomic force microscopy (AFM) indicated 2.5-3.0 nm heights, reflecting a bilayer structure comprised of two molecules of **1**-SP, which exhibit extended lengths of ~1.6 nm (Figs. 3e-f, S3).

Accordingly, the ideal reaction conditions to perform the aldol reaction under dynamic conditions with a high k_{on}/k_{off} ratio utilized 5 mole % **1**, 50 mM formic acid, and a 5-fold excess of cyclohexanone in water at 60°C. Using these optimized conditions under static conditions at 60° C for 8 h, the reaction proceeded to ~90% completion under irradiation with visible light; whereas, the catalyst remained dormant in the dark and the reaction only proceeded to ~5 % conversion (Fig 4 b). A transient catalytic reaction was then explored at 60°C in which the light was turned on and off in 2 h intervals over 8 h. Monitoring the progress of the reactions over two "on-off" cycles of light showed a steep rise in conversion under light-on conditions that

This journal is © The Royal Society of Chemistry 20xx

Please do not adjust margins

was immediately attenuated when the light source was extinguished (Fig. 4a).

In conclusion, we have demonstrated the dissipative self-assembly of a Pro-Lys dipeptide, **1**, into a catalytic nanosheet that promoted the aldol reaction in the presence of visible light. Transient catalytic activity for the aldol reaction emerged from **1** under light illumination due to the photoisomerization of the *O*-protonated (**1**-MCH$^+$) form to the spiropyran (**1**-SP) state, which rapidly assembled into nanosheets capable of catalyzing the aldol reaction in water. When the light source was removed, thermal isomerization to the more stable MCH$^+$ form caused the nanosheets to dissociate into a catalytically inactive, monomeric state. Efficient deactivation of the catalyst under light-off conditions required performing the reaction at 60°C to ensure rapid SP→MCH$^+$ isomerization. At higher temperatures, the k_{on}/k_{off} ratio was maximized by replacing the trifluoracetates that were ion-paired with the ammonium side chains of **1** with less lipophilic formate counterions. Under these conditions, the aldol reaction could be repeatedly activated and deactivated by switching the light source on and off. The ability to regulate catalytic activity represents an important step toward the development of larger, networked systems with spatial and temporal control of reactivity and function.

Acknowledgements

This material is based upon work supported by the National Science Foundation (CHE-2106924).

Notes and references

1. C. M. Agapakis, P. M. Boyle and P. A. Silver, *Nat. Chem. Biol.*, 2012, **8**, 527-535.
2. A. H. Chen and P. A. Silver, *Trends. Cell Biol.*, 2012, **22**, 662-670.
3. P. Goloubinoff, A. S. Sassi, B. Fauvet, A. Barducci and P. De Los Rios, *Nat. Chem. Biol.*, 2018, **14**, 388-395.
4. E. Karsenti, *Nat. Rev. Mol. Cell Bio.*, 2008, **9**, 255-262.
5. B. A. Grzybowski, K. Fitzner, J. Paczesny and S. Granick, *Chem. Soc. Rev.*, 2017, **46**, 5647-5678.
6. S. A. P. van Rossum, M. Tena-Solsona, J. H. van Esch, R. Eelkema and J. Boekhoven, *Chem. Soc. Rev.*, 2017, **46**, 5519-5535.
7. E. Mattia and S. Otto, *Nat. Nanotechnol.*, 2015, **10**, 111-119.
8. S. De and R. Klajn, *Adv. Mater.*, 2018, **30**, e1706750.
9. B. Rieß, R. K. Grötsch and J. Boekhoven, *Chem.*, 2020, **6**, 552-578.
10. F. Della Sala, S. Neri, S. Maiti, J. L. Chen and L. J. Prins, *Curr. Opin. Biotechnol.*, 2017, **46**, 27-33.
11. J. Deng and A. Walther, *J. Am. Chem. Soc.*, 2020, **142**, 685-689.
12. S. Dhiman, A. Jain, M. Kumar and S. J. George, *J. Am. Chem. Soc.*, 2017, **139**, 16568-16575.
13. J. Boekhoven, W. E. Hendriksen, G. J. M. Koper, R. Eelkema and J. H. van Esch, *Science*, 2015, **349**, 1075.
14. S. Debnath, S. Roy and R. V. Ulijn, *J. Am. Chem. Soc.*, 2013, **135**, 16789-16792.
15. I. Maity, N. Wagner, R. Mukherjee, D. Dev, E. Peacock-Lopez, R. Cohen-Luria and G. Ashkenasy, *Nat. Commun.*, 2019, **10**, 4636.
16. W. A. Ogden and Z. Guan, *ChemSystemsChem*, 2019, **2**.
17. C. Sharma and A. Walther, *Angew. Chem. Int. Ed.*, 2022, **61**, e202201573.
18. Y. Wei, S. Han, J. Kim, S. Soh and B. A. Grzybowski, *J. Am. Chem. Soc.*, 2010, **132**, 11018-11020.
19. M. Cortes-Clerget, N. Akporji, J. Zhou, F. Gao, P. Guo, M. Parmentier, F. Gallou, J. Y. Berthon and B. H. Lipshutz, *Nat. Commun.*, 2019, **10**, 2169.
20. S. Maiti, I. Fortunati, C. Ferrante, P. Scrimin and L. J. Prins, *Nat. Chem.*, 2016, **8**, 725-731.
21. X. Lang, U. Thumu, L. Yuan, C. Zheng, H. Zhang, L. He, H. Zhao and C. Zhao, *Chem. Commun.*, 2021, **57**, 5786-5789.
22. S. Chandrabhas, S. Maiti, I. Fortunati, C. Ferrante, L. Gabrielli and L. J. Prins, *Angew. Chem. Int. Ed.*, 2020, **59**, 22223-22229.
23. M. A. Cardona and L. J. Prins, *Chem. Sci.*, 2019, **11**, 1518-1522.
24. H. Zhao, S. Sen, T. Udayabhaskararao, M. Sawczyk, K. Kucanda, D. Manna, P. K. Kundu, J. W. Lee, P. Kral and R. Klajn, *Nat. Nanotechnol.*, 2016, **11**, 82-88.
25. R. Chen, S. Neri and L. J. Prins, *Nat. Nanotechnol.*, 2020, **15**, 868-874.
26. M. Szewczyk, G. Sobczak and V. Sashuk, *ACS Catal.*, 2018, **8**, 2810-2814.
27. R. L. Lawrence, B. Scola, Y. Li, C. K. Lim, Y. Liu, P. N. Prasad, M. T. Swihart and M. R. Knecht, *ACS Nano.*, 2016, **10**, 9470-9477.
28. K. S. Lee and J. R. Parquette, *Chem. Commun.*, 2015, **51**, 15653-15656.
29. B. List, R. A. Lerner and C. F. Barbas, *J. Am. Chem. Soc.*, 2000, **122**, 2395-2396.
30. F. Rodriguez-Llansola, J. F. Miravet and B. Escuder, *Chem. Commun.*, 2009, 7303-7305.
31. T. He, K. Li, M.-Y. Wu, M.-B. Wu, N. Wang, L. Pu and X.-Q. Yu, *Tetrahedron*, 2013, **69**, 5136-5143.
32. A. Patti and S. Pedotti, *Eur. J. Org. Chem.*, 2014, **2014**, 624-630.
33. L. Zhong, Q. Gao, J. B. Gao, J. L. Xiao and C. Li, *J. Catal.*, 2007, **250**, 360-364.
34. M. Liu, C. N. Creemer, T. J. Reardon and J. R. Parquette, *Chem. Commun.*, 2021, **57**, 13776-13779.
35. R. Klajn, *Chem. Soc. Rev.*, 2014, **43**, 148-184.
36. Y. Shiraishi, M. Itoh and T. Hirai, *Phys. Chem. Chem. Phys.*, 2010, **12**, 13737-13745.
37. G. D. Yadav, Deepa and S. Singh, *ChemistrySelect*, 2019, **4**, 5591-5618.
38. M. Shibue, C. T. Mant and R. S. Hodges, *J. Chromatogr. A*, 2005, **1080**, 68-75.
39. C. L. Shen, M. C. Fitzgerald and R. M. Murphy, *Biophys. J.*, 1994, **67**, 1238-1246.
40. T. C. Nugent, A. E. Vos, I. Hussain, H. A. El Damrany Hussein and F. Goswami, *Eur. J. Org. Chem.*, 2022, **2022**.